Tanzania Journal of Science 50(4): 912-920, 2024
ISSN 0856-1761, e-ISSN 2507-7961

First-Principles studies on the Electronic and Optical Properties of Corundum samples from the Tanga region

Esther J. Tarimo*, Pulapa V Kanaka Rao and F.M. Stanley
Department of Physics, College of Natural and Mathematical Sciences,
University of Dodoma, P. O. Box 338 Dodoma, Tanzania
**Corresponding author. Email: esthertarimoj@gmail.com*
Telephone: +255 766 615 693
Received 8th Aug. 2024, Reviewed 30th Aug., Accepted 27th Oct., Published 30th Nov. 2024
https://dx.doi.org/10.4314/tjs.v50i4.16

Abstract

The characteristics of corundum are significant as they provide accurate identification supporting its diverse applications, facilitating the development of advanced materials, and ensuring its optimal use across various fields. Corundum alumina (α-Al_2O_3) samples collected from the Tanga mining region were characterized for crystallographic information using XRD analysis. This crystallographic information was used to build the crystal system of the sample in Biovia Materials Studio modelling and simulation software. The electrical and optical properties of this sample were examined by applying first-principles density functional theory and Generalized Gradient Approximations. For the calculations, a sampling mesh of 6×6×2 k-points, with an energy cut-off of 600 eV, and an energy convergence within 1.0 x 10^{-5} eV/atom were used. The band gap determined is 6.34 eV at the gamma point exhibiting an insulating property. By plotting their polarized dielectric function in various directions, the optical properties were evaluated. The reflectivity spectra exhibited anisotropic behaviour in the ultraviolet region, enhancing its performance in various electronic and photonic applications. Also, the absorption peaks observed are 64.81 nm along [001] crystalline direction and 65.29 nm along [100] and [010] crystalline directions.

Keywords: First-Principles studies; Corundum; Band gap; Polarized and anisotropic reflectivity

Introduction

Due to various environmental factors, corundum is aluminium oxide (Al_2O_3) and exhibits distinct properties (Aggarwal and Ramdas 2019). It is a naturally occurring mineral with geologically derived characteristics, and it can only be found in a few places worldwide (Keulen et al. 2020). Sri Lanka, Myanmar, Tanzania, Kenya, Madagascar, Australia, and Mozambique are among the nations that have significant natural corundum resources (Mansoor et al. 2021). Tanzania, on the other hand, is worth noting for being home to the largest corundum reserve in Africa (Park 2004). For quantitative evaluation of the corundum stone to be used by gemmologists, the stone industry, manufacturing industries, and the medical field, the corundum stone's characteristics are useful (Raisin et al. 2021). It is vital to use different techniques to comprehend the electrical and optical properties because they are a well-known necessity for their technological applications.

However, the advancements in density functional theory (DFT), a computational approach, now allow us to explore the electrical structure at a microscopic level (Ozaki et al. 2021). The plane wave pseudopotential approach, which derives the properties of materials from their fundamental principles, is used in the DFT

using the Cambridge Serial Total Energy Package (CASTEP). Numerous material properties, such as energetics, electrical response properties, vibrational properties, and atomic-level structure, can be simulated using computational methods (Kovilpalayam et al. 2022). The present study aimed to understand the electronic properties and optical anisotropic properties of corundum samples from the Tanga mining region at the microscopic level by the DFT method. The structural parameters obtained from the XRD analysis were used to build the crystal structure that was used in computing the electronic and optical properties using the first principles of density functional theory.

Gemstone applications are not just restricted to jewellery (Akbudak et al. 2021). Moreover, gemstones have diverse applications such as glass cutting tools and quartz's piezoelectricity for electrical circuits. However, the majority of the existing and prevalent grading methods rely on human visual inspection, which eventually results in error (Rahalim et al. 2021). The gem varieties of corundum: ruby and sapphire have attracted a great deal of scientific interest. In which, the main focus areas of study have been mineral deposits, mineral age and origin, the colour variations related to impurities present, mineralogical, crystallographic, physical properties, fluorescence and their use as gemstones (Jeršek et al. 2021). Mohsin et al. (2021) highlight the substantial impact of the mining industry on economic development. Furthermore, research in structural mineralogy and crystallography, as emphasized by Krivovichev (2017), capitalizes on efforts to elucidate the atomic configurations of gemstones. Thus, this study aimed to understand the electronic and optical properties of corundum samples from the Tanga region at the microscopic level by using the DFT method.

Methodology

XRD analysis was conducted on commercial corundum samples obtained from the Tanga mining region. At ambient temperature, using a Bruker AXS D76187 X-ray powder diffractometer in step scanning setting of 0.02° (2θ), a Cu pipe of λ = 1.540598 and an estimation time of 0.15 s per step, the diffraction lines of the samples were captured. The diffraction lines of the samples were captured and recorded within a scanning interval of 5^0 – 65^0 (2θ). The structural parameters obtained from XRD analysis were used to build the crystal system of the sample in Biovia material studio modelling and simulation software. Then density functional analysis was performed by applying the Cambridge Sequential Total Energy Package (CASTEP) method (Perdew and Wang 1992), with the Perdew-Burke-Ernzerhof (PBE) paradigm and generalized gradient approximation (GGA) for the transfer association function (Perdew et al. 1996). To guarantee an overall energy convergence, a sampling mesh of 6×6×2 special Monkhorst-Pack k-points, with the cut-off energy of 600 eV, and the total energy convergence within 1.0 x 10^{-5} eV/atom were implemented (Vanderbilt 1990). The pseudopotential configurations, $3s^2$ $3p^1$ electrons for the Al atom and $2s^2$ $2p^4$ electrons for O atoms were implemented. This allows efficient, accurate and minimization of the computational cost (Clark and Robertson 2010). Furthermore, the electronic and optical properties were computed using density functional theory implemented in CASTEP with the GGA technique. The evaluation of the computed electrical and optical characteristics in this study was compared with theoretical and experimental values available in the literature.

Results and Discussion

Structural properties

A trigonal Bravais structure on a space group R3c and the hexagonal unit cell in Figure 1 are inferred from the XRD spectra having the lattice parameters, which are comparable with theoretical information (Sawada 1994 and Giuliani et al. 2020). The positions of atoms in Figure 1 are (0.2945, 0, 0.25) and (0, 0, 0.3515) for Al and O, respectively. As seen in Table 1, the optimized parameters are also comparable to

both experimental results and theoretical values (Sawada 1994). However, some deviations observed are proposed to be caused by variations in the crystal's growth conditions, impurity concentrations and geological processes since the samples are from different geological environments. Figure 2 depicts the XRD patterns for experimental and simulation as observed from the same 2θ degree. The XRD patterns obtained by the material studio (simulated results) are almost like the experimental one, with slight differences in small peaks that were captured by XRD. The small peaks that are seen in the XRD patterns might be attributed to the background noise due to impurities, crystal defects and surface contaminations. It may also be contributed by very little number of other metals constituents like Mg, Si, Ti, V, Cr, Fe, Ga, K and Mn that might be present in the sample (Dubinsky et al. 2020).

Table 1: Structural parameters

Hexagonal	Experimental values (this work)	Optimized values (this work)	Theoretical values (Sawada 1994)
a (Å)	4.7582	4.7446	4.7589
c (Å)	12.9897	13.0001	12.9919
D (g/cm^2)	3.989	4.008	3.9860
V (Å^3)	254.692	253.437	254.810

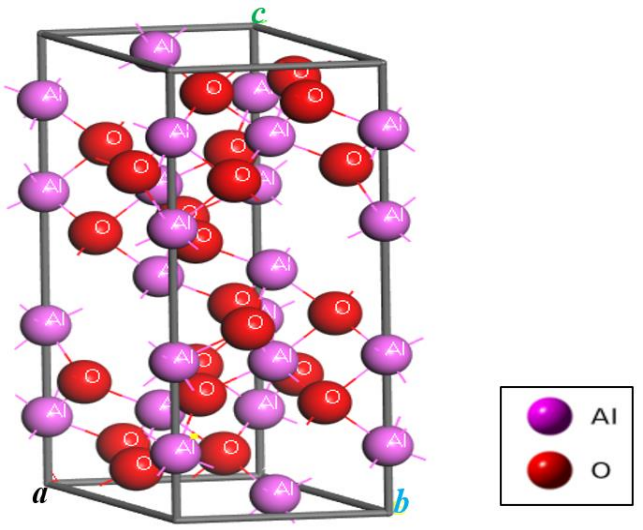

Figure 1: Tanga mining site Corundum's crystal structure in hexagonal lattice

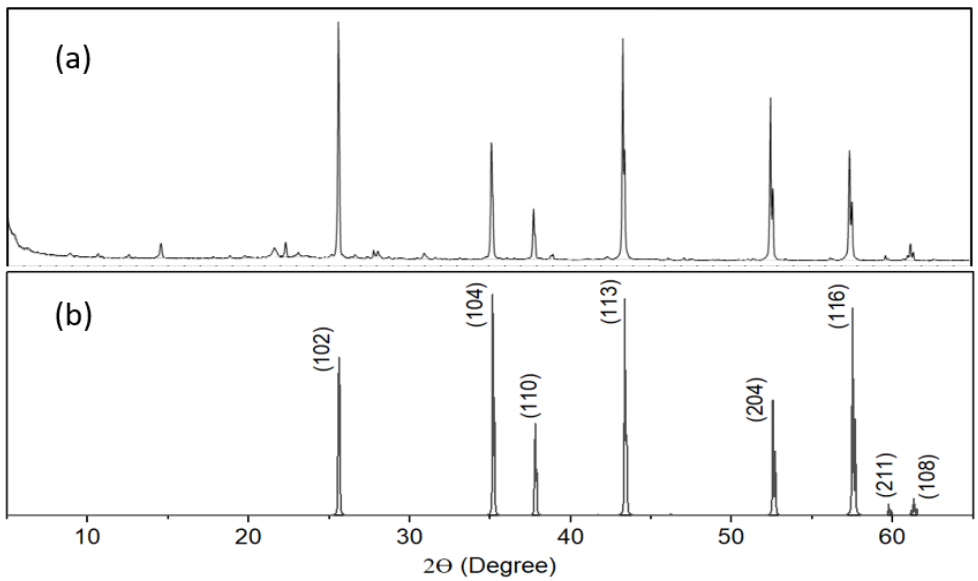

Figure 2: XRD pattern for the Tanga sample (a) experimental and (b) simulated.

Electronic properties of corundum

The band arrangement and density of states for the Al_2O_3 sample are presented in Figure 3(a & b). From Figure 3 (a), it is observed that the corundum samples exhibited a direct bandgap with an estimated value of 6.34 eV obtained at the gamma point. It is worth noting that this value lies within a variety of prior discoveries and experimental values of 6 eV-9.5 eV (Zainullina and Korotin 2020). The density of states in Figure 3(b) is obtained from the contributions of O2p (−7.8 eV-0 eV), Al3s (6.34 eV-19.11 eV), and Al3p (6.78 eV-20.09 eV). These values are described in Figure 4 (b & c), and Figure 4 (a) shows the contributions of the total density of the state. It is clearly that the bandgap of corundum from Tanga is an insulator in character.

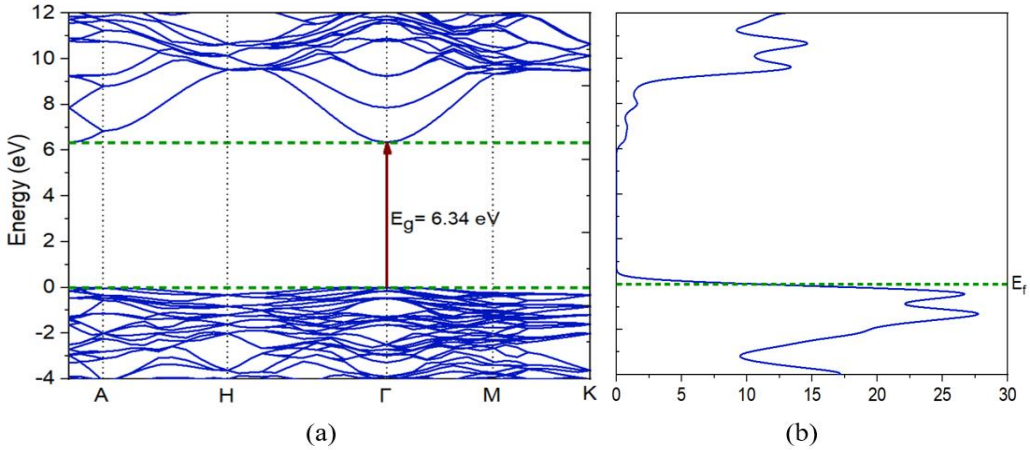

Figure 3: Simulated sample for Corundum (a) band structure and (b) density of states

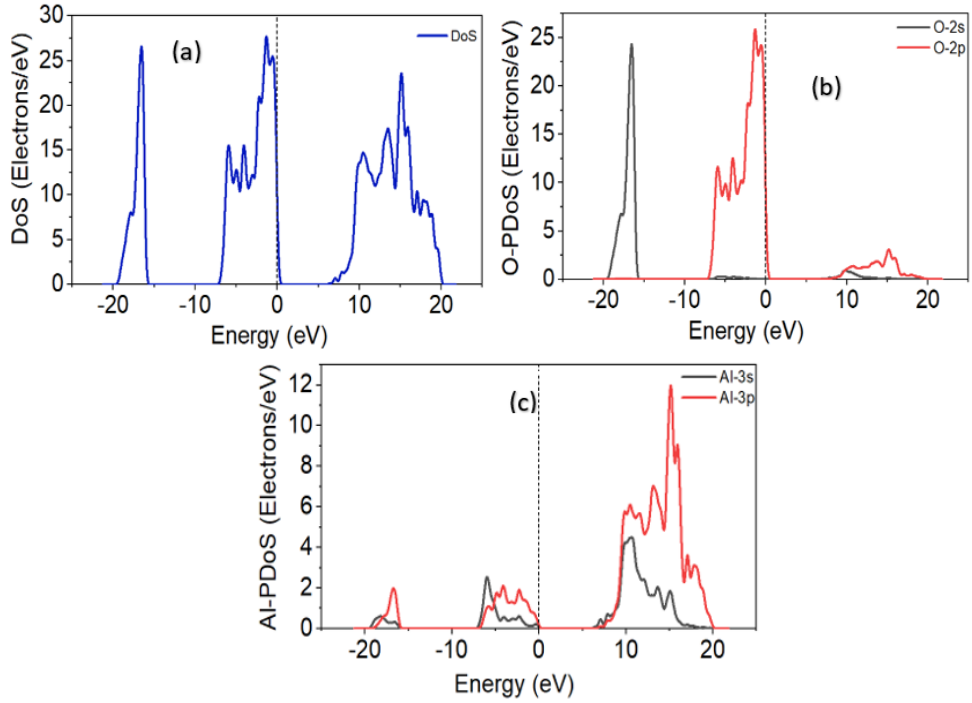

Figure 4: Simulated sample (a) total density of state, (b) O-partial density of state (b) and (c) Al-partial density of state

Optical properties

A deep understanding of the electronic structure of materials is provided by optical functions such as the absorption coefficient, α(ω); refractive index, *n*(ω); the extinction coefficient, k(ω); reflectivity, R(ω); and energy loss function, L(ω) (Karazhanov et al. 2007). The dielectric function, which describes an electronic system's linear response when an external electric field is present, is given by equation (1) as used elsewhere (Khireddine et al. 2021). The dielectric function is a useful parameter for characterizing the optical properties of materials.

$$\varepsilon(\omega) = \varepsilon_1(\omega) + i\varepsilon_2(\omega) \quad (1)$$

Where: $\varepsilon_1(\omega)$ is the real part and $\varepsilon_2(\omega)$is the imaginary part. The real ε_1 and imaginary ε_2 parts are calculated using equations (2) and (3). These values are important because all other parameters of optical properties can be deduced from those two values as presented in equations (4) – (8) (Heiba et al. 2020):

$$\varepsilon_1(\omega) = 1 + \frac{2p}{\pi}\int_0^{\infty} \frac{\omega'}{\omega^{0.2} - \omega^2} d\omega' \quad (2)$$

$$\varepsilon_2(\omega) = \frac{2\omega p}{\pi}\int_0^{\infty} \frac{\varepsilon_1 - 1}{\omega^{0.2} - \omega^2} d\omega' \quad (3)$$

$$\alpha(\omega) = \sqrt{2\omega}\sqrt{(\varepsilon_1^2 + \varepsilon_2^2)^{\frac{1}{2}} - \varepsilon_1} \quad (4)$$

$$n(\omega) = \sqrt{\frac{\varepsilon_r(\omega)}{2} + \frac{(\varepsilon_r^2(\omega) + \varepsilon_i^2(\omega))^{1/2}}{2}} \quad (5)$$

$$k(\omega) = \sqrt{\frac{-\varepsilon_r(\omega)}{2} + \frac{(\varepsilon_r^2(\omega) + \varepsilon_i^2(\omega))^{1/2}}{2}} \quad (6)$$

$$R(\omega) = \frac{(n-1)^2 + K^2}{(n+1)^2 + K^2} \quad (7)$$

$$L(\omega) = \frac{\varepsilon_2(\omega)}{\varepsilon_1^2(\omega) + \varepsilon_2^2(\omega)} \quad (8)$$

Figure 5(a & b) shows the dielectric function spectra of the real (ε_1) and imaginary (ε_2) sections of the dielectric characteristics, respectively. As seen in

Figure 5 (a), the real component of dielectric absorption has the first peak at 10.25. The static dielectric constant ε_1 (0) is determined when the frequency is zero, which is linked with the bandgap of the rear portion. From this, the ordinary refractive index can be calculated as given in equation (9).

$$n(0) = \varepsilon(0)^{\frac{1}{2}} \qquad (9)$$

The estimated static dielectric constant ε_1 (0) for the corundum sample is 3.05 (Figure 5 a), when the value of the ordinary refractive index of 1.746 is obtained. This estimated value of the ordinary refractive index obtained using Figure 5 (a) coincides with the one in Figure 5 (c). The refractive index obtained in this study is comparable to the refractive index of 1.774 from the analysis of α-Al_2O_3 (Zouboulis and Grimsditch 1991). This value of refractive index is greater than that of glass, which implies that the material considered in this study is not a glass. The imaginary portion of the dielectric function and extinction coefficient are also displayed in Figure 5 (b & d). The results show a good agreement for spectra with the theoretical study by (Feneberg et al. 2018). Therefore, it can be considered as the results that form the basis for further studies.

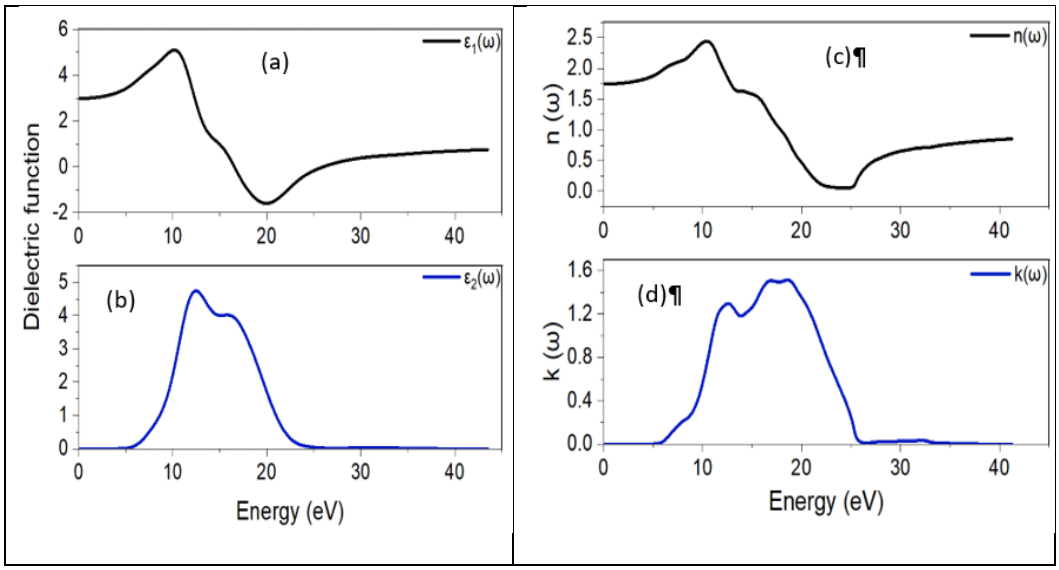

Figure 5: (a) Real part of dielectric function (b)Imaginary part of dielectric function (c) Refractive index (d) and Extinction coefficient

Figure 6 represents the variations of reflectivity, absorption coefficient, and loss function. As depicted in Figure 6 (a), the maximum peak of reflectivity is at 53 nm for the [001] direction, whereas along [010] and [100] directions, the maximum peak reflectivity was observed at 49 nm. This indicates that the reflectivity is anisotropic, a significant property in designing advanced optical systems, enhancing gemstone aesthetics, and developing specialized devices for various industries. Figure 6 (b) indicates the maximum peak for the absorption coefficient, which was around 64.81 nm and 74.51 nm along [001] directions, while the peak was around 65.29 nm along [010] and [100] directions, respectively. The sample volume, population of energy levels, and molecular rotation all of which vary depending on the location are what cause the peaks to be visible. The energy loss spectrum shows how much energy is lost when a rapid electron moves through the material (Bouhemadou and

Khenata 2007). The bulk plasma frequency ω_p is the main peak on the loss function spectrum; this happens as $\varepsilon_2 < 1$ and ε_1 approach zero (Li et al. 2008). The quick decline of the reflectance indicated in Figure 6(a) agrees with the sharp peak loss function observed in Figure 6(c). The value of the primary peak in the loss function is approximated to be 26.5 eV (Figure 6 c), providing valuable information about this selected sample's electronic structure, band gap, and optical properties. However, it paves the way to gain insight into the designing of different materials for specific applications from the selected sample.

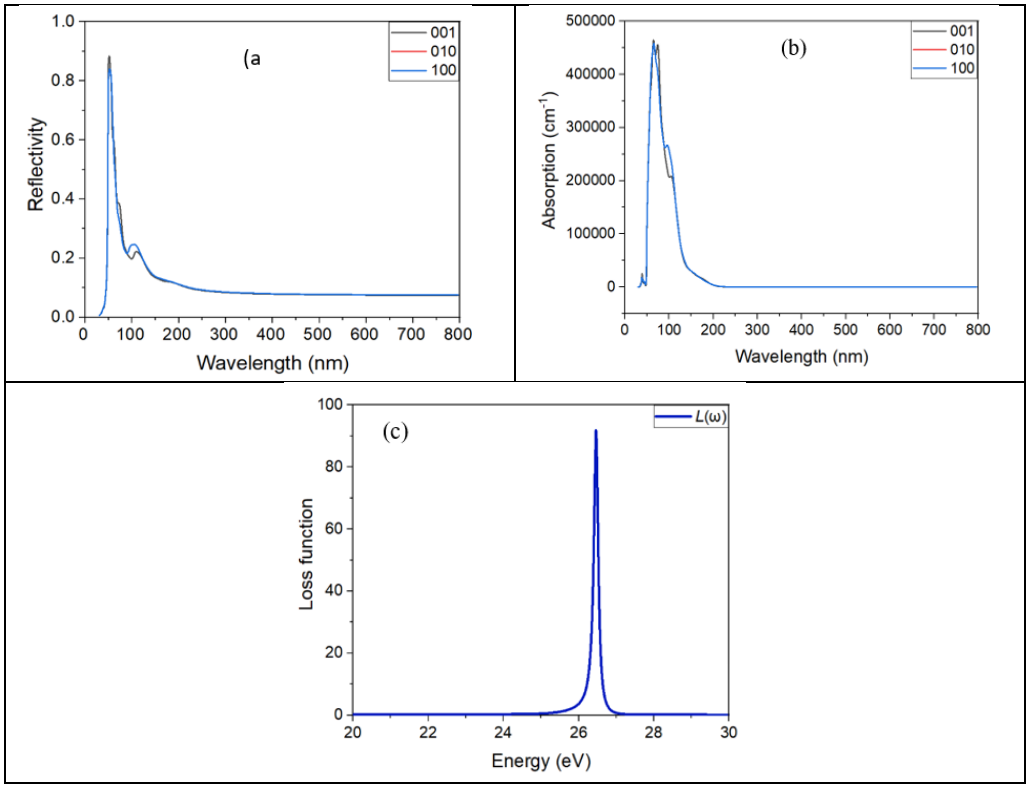

Figure 6: (a) Reflectivity (b) Absorption coefficient (c), and Loss function

Conclusion

We used the first principles study technique to report the findings of electronic and optical characteristics of α–Al_2O_3 in the corundum gemstones from the Tanga mining region. Our findings correlated well with the known theoretical and experimental values. From the findings, the reflectivity spectra showed anisotropic behaviour in the UV region. Furthermore, the results indicated that the selected corundum sample is a suitable insulator described by a band gap of 6.34 eV. There are still minor variations between the estimated optical spectra and the theoretical values available in the literature, despite their good agreement. To gain a deep insight into corundum gemstone from the Tanga mining region on the electrical and optical properties the interaction between electrons can further be studied using other computational techniques and experimental.

Acknowledgement

The authors gratefully acknowledge the Twiga Cement Industry for their assistance during XRD analysis and the Department of

Physics at the University of Dodoma for their contributions during the conceptualization of the idea.

Conflict of Interest

The authors confirm that they are free of any conflicts of interest.

References

Aggarwal RL and Ramdas AK 2019 *Physical properties of diamond and sapphire*. CRC Press.

Akbudak İK, Gurbuz M, Basibuyuk Z, Hatipoglu M, Önal AÖ and İsler F 2021 Mineralogical And Gemological Characteristics Of Metaophiolite Hosted Corundum (Malatya-Türkiye). *SAUJS*. 25(2): 288-296.

Bouhemadou A and Khenata R 2007 Ab initio study of the structural, elastic, electronic and optical properties of the antiperovskite SbNMg3. *Comput. Mater. Sci*. 39(4): 803-807.

Clark SJ and Robertson J 2010 Screened exchange density functional applied to solids. *Phys. Rev. B*. 82(8): 085208.

Dubinsky EV, Stone-Sundberg J and Emmett JL 2020 A quantitative description of the causes of color in corundum. *Gems Gemol*. 56(1): 1-27.

Feneberg M, Nixdorf J, Neumann MD, Esser N, Artús L, Cuscó R, Yamaguchi T and Goldhahn R 2018 Ordinary dielectric function of corundumlike α− Ga_2O_3 from 40 meV to 20 eV. *Phys. Rev. Mater*. 2(4): 044601.

Giuliani G, Groat LA, Fallick AE, Pignatelli I and Pardieu V 2020 Ruby deposits: A review and geological classification. *Minerals*. 10(7): 597.

Heiba Z, Mohamed MB and Wahba AM 2020 Structural, optical, mechanical, and electronic properties of Cr-doped alumina. *J. Mater. Sci.: Mater. Electron*. 31: 14645-14657.

Jeršek M, Jovanovski G, Boev B and Makreski P 2021 Intriguing minerals: corundum in the world of rubies and sapphires with special attention to Macedonian rubies. *ChemTexts*. 7(3): 1-23.

Karazhanov SZ, Ravindran P, Kjekshus A, Fjellvåg H and Svensson B 2007 Electronic structure and optical properties of Zn X (X= O, S, Se, Te): A density functional study. *Phys. Rev. B.* 75(15): 155104.

Keulen N, Thomsen TB, Schumacher JC, Poulsen MD, Kalvig P, Vennemann T and Salimi R 2020 Formation, origin, and geographic typing of corundum (ruby and pink sapphire) from the Fiskenæsset complex, Greenland. *Lithos*. 366: 105536.

KhireddineA , Bouhemadou A, Alnujaim S, Guechi N, Bin-Omran S, Al-Douri Y, Khenata R, Maabed S and Kushwaha A 2021 First-principles predictions of the structural, electronic, optical and elastic properties of the zintl-phases AE3GaAs3 (AE= Sr, Ba). *Solid State Sci*. 114: 106563.

Kovilpalayam PD, Arumugan P, Munusami R, Chinnasamy A, Madhu S, Paulraj P and Palani K 2022 First Principles Study on Electronic Structure and Optical Properties of PMMA Doped InSb–Mn Alloy Polymer Matrix Composite. *Adv. Mater. Sci. Eng. 2022*.

Krivovichev SV 2017 Structure description, interpretation, and classification in mineralogical crystallography. *Crystallogr. Rev.* 23(1): 2-71.

Li C, Wang B, Wang R, Wang H and Lu X 2008 First-principles study of structural, elastic, electronic, and optical properties of orthorhombic BiGaO3. *Comput. Mater. Sci. 42*(4): 614-618.

Mansoor M, Mansoor M, Mansoor M, Themelis T and Şahin FÇ 2021 Sintered transparent polycrystalline ceramics: the next generation of fillers for clarity enhancement in corundum. *Synth. Sinter*. 1(3): 183-188.

Mohsin M, Zhu Q, Naseem S, Sarfraz M and Ivascu L 2021 Mining industry impact on environmental sustainability, economic growth, social interaction, and public health: an application of semi-quantitative mathematical approach. *Processes*. *9*(6): 972.

Ozaki Y, Beć KB, Morisawa Y, Yamamoto S, Tanabe I, Huck CW and Hofer TS 2021 Advances, challenges, and perspectives of quantum chemical approaches in molecular

spectroscopy of the condensed phase. *Chem. Soc. Rev.* 50(19): 10917-10954.

Park H 2004 The gemological study of ruby and sapphire from Tanzania Msc Thesis, *Pukyong National University*. Korea, p.1-7.

Perdew JP, Burke K and Ernzerhof M 1996 Generalized gradient approximation made simple. *Phys. Rev. Lett. 77*(18): 3865.

Perdew JP and Wang Y 1992 Accurate and simple analytic representation of the electron-gas correlation energy. *Phys. Rev. B*. 45(23): 13244.

Rahalim FM, Jamaludin J, Raisin SN, Ismail I, Wahab YA, Rahim RA, Sahrim M, Balakrishnan SR, Ismail WZW and Mohamad FAJ 2021 Analysis on Clarity of Rubies Gemstones Using Charge-Coupled Device (CCD). *TSSA.* Vol: 4(1).

Raisin SN, Jamaludin J, Ismail I, Wahab YA, Rahim RA, Balakrishnan SR, Ismail WZW, Rahalim FM, Jamal FAM and Zaini NAHS 2021 Simulation Study on CCD Tomography System for Ruby Stone Optical Properties. *TSSA.* 1(4).

Sawada H 1994 Residual electron density study of α-aluminum oxide through refinement of experimental atomic scattering factors. *Mater. Res. Bull.* 29(2): 127-133.

Vanderbilt D 1990 Soft self-consistent pseudopotentials in a generalized eigenvalue formalism. *Phys. Rev. B. 41*(11): 7892.

Zainullina VM and Korotin MA 2020 Regulation of corundum band gap width by p elements and vacancy co-doping. *J. Phys. Chem. Solids.* 140: 109357.

Zouboulis E and Grimsditch M 1991 Refractive index and elastic properties of single-crystal corundum (α-Al2O3) up to 2100 K. *J. Appl. Phys.* 70(2): 772-776.